Acta Cryst. (1999). B**55**, 17–23

Neutron structures of ammonium tetrafluoroberyllate

R. C. Srivastava,[a] W. T. Klooster[b] and T. F. Koetzle[b]*

[a]*Department of Physics, Indian Institute of Technology, Kanpur 208016, India, and* [b]*Chemistry Department, Brookhaven National Laboratory, PO Box 5000, Upton, NY 11973, USA. E-mail: koetzle@glx.chm.bnl.gov*

(*Received 30 June 1997; accepted 27 May 1998*)

Abstract

It is thought that hydrogen bonding is responsible for the ferroelectricity in ammonium tetrafluoroberyllate, $(NH_4)_2BeF_4$. In the past X-ray data have been collected, but these did not permit accurate determination of the H-atom positions. In order to obtain more accurate information the neutron structures have now been determined for the paraelectric and ferroelectric phases. Going from the paraelectric to the ferroelectric phase, both the BeF_4^{2-} and the NH_4^+ ions rotate and shift from the mirror planes of the paraelectric phase. This results in removal of the mirror-plane symmetry and formation of a superlattice with the *a* axis doubled. Along the polar *c* axis, the NH_4^+ ions move towards the BeF_4^{2-} ions within chains of molecules and the chains move slightly relative to one another. The rotations and translations give rise to stronger hydrogen-bonding interactions.

1. Introduction

The room-temperature phase of ammonium tetrafluoroberyllate (AFB) is paraelectric with space group *Pnma*. AFB undergoes a nonferroelectric transition at 182 K (Strukov *et al.*, 1973; Makita & Yamauchi, 1974) to a phase that is incommensurate along the *a* axis with a period of $\sim 2a$ (Iizumi & Gesi, 1977). A ferroelectric transition occurs at 175 K (Pepinsky & Jona, 1957). In the ferroelectric phase the *a* axis is doubled compared with the paraelectric phase and the space group is $Pna2_1$. Several investigators have measured physical properties, including spontaneous polarization (Hoshino *et al.*, 1958), dielectric behavior (Strukov *et al.*, 1962; Ohshima & Nakamura, 1966) and changes in activation energies through the phase transition (O'Reilly *et al.*, 1967). An improper ferroelectric model has been proposed (Levanyuk & Sannikov, 1969), but the mechanism of the phase transition is not clear. O'Reilly *et al.* (1967) suggest that one of the two independent ammonium ions in the unit cell becomes ordered in the ferroelectric phase and the transition is of order–disorder type. However, deuterated AFB samples show almost no change in the activation energies of ammonium ions on going through the phase transition (Kydon *et al.*, 1969). Onodera & Shiozaki (1979) report some disorder in one of the two independent ammonium ions in the paraelectric phase of AFB and also fairly dissimilar distortions in the four symmetry-nonequivalent ammonium ions in the structure at 133 K after going through the ferroelectric phase transition. They also suggest that the two ammonium ions that result from the ordering of the ion that they find to be disordered in the paraelectric phase take antiparallel up and down states along the ferroelectric polar axis with the consequent loss of the mirror symmetry. This occurs because of stronger hydrogen bonding and resulting restricted freedom in the ferroelectric phase. They do, however, suggest more accurate dielectric and diffraction experiments. According to Garg & Srivastava (1979), the X-ray crystal structure of AFB in the paraelectric phase *does not* indicate any disorder in the ammonium ions. These authors, like Onodera & Shiozaki (1979), conclude that ferroelectricity in AFB most probably results from changes in hydrogen bonding. In order to obtain more accurate H-atom positions, the neutron structures have now been determined for the paraelectric and ferroelectric phases.

2. Experimental

From a large crystal (approximately $1.5 \times 1.0 \times 0.5$ cm), provided by Professor Y. Ono of Tohoku University, Japan, a piece was cut and mounted on an aluminium pin with halocarbon grease (Dow–Corning), sealed in an aluminium container under a helium atmosphere, and placed in a DISPLEX Model CS-202 closed-cycle refrigerator (APD Cryogenics Inc.). Neutron diffraction data were obtained on the four-circle diffractometer at beam port H6M of the High Flux Beam Reactor at Brookhaven National Laboratory at 200, 163 and 20 K. The neutron beam, monochromated by Be(002) planes in reflection geometry, had a wavelength of 1.0462 (1) Å, as calibrated against a KBr crystal (a_o = 6.6000 Å at 295 K). The intensities of two reflections were monitored periodically as a check on the experimental stability and these showed no systematic variation throughout. The crystal temperature was maintained within ±0.5 K during each experiment. The unit cells were determined by a least-squares fit of $\sin^2\theta$ values for 32 reflections in the range $20 < 2\theta < 27°$. Intensity data were measured over one octant by means of $\theta/2\theta$ step

© 1999 International Union of Crystallography
Printed in Great Britain – all rights reserved

Table 1. *Experimental details*

	200 K	163 K	20 K
Crystal data			
Chemical formula	$(NH_4)_2BeF_4$	$(NH_4)_2BeF_4$	$(NH_4)_2BeF_4$
Chemical formula weight	121.093	121.093	121.093
Cell setting	Orthorhombic	Orthorhombic	Orthorhombic
Space group	*Pnma*	$Pna2_1$	$Pna2_1$
a (Å)	7.531 (3)	15.017 (6)	14.997 (5)
b (Å)	5.874 (2)	5.876 (3)	5.860 (3)
c (Å)	10.399 (4)	10.418 (4)	10.402 (4)
V (Å^3)	460.0 (5)	919.2 (12)	914.1 (11)
Z	4	8	8
D_x (Mg m^{-3})	1.748	1.750	1.759
Radiation type	Neutron	Neutron	Neutron
Wavelength (Å)	1.0462	1.0462	1.0462
No. of reflections for cell parameters	32	32	32
θ range (°)	20–27	20–27	20–27
μ (mm^{-1})	0.291	0.291	0.293
Temperature (K)	200	163	20
Crystal form	Box	Box	Box
Crystal size (mm)	4.0 × 3.9 × 3.9	4.0 × 3.9 × 3.9	4.0 × 3.9 × 3.9
Crystal color	Colorless	Colorless	Colorless
Data collection			
Diffractometer	Beamline H6M, HFBR	Beamline H6M, HFBR	Beamline H6M, HFBR
Data collection method	$\theta/2\theta$ scans	$\theta/2\theta$ scans	$\theta/2\theta$ scans
Absorption correction	Analytical	Analytical	Analytical
T_{min}	0.356	0.346	0.343
T_{max}	0.428	0.432	0.431
No. of measured reflections	1018	1972	1516
No. of independent reflections	996	1932	1484
No. of observed reflections	790	1390	1363
Criterion for observed reflections	$I > 3\sigma(I)$	$I > 3\sigma(I)$	$I > 3\sigma(I)$
θ_{max} (°)	55	55	55
Range of h, k, l	$0 \rightarrow h \rightarrow 11$ $0 \rightarrow k \rightarrow 9$ $0 \rightarrow l \rightarrow 16$	$0 \rightarrow h \rightarrow 23$ $0 \rightarrow k \rightarrow 9$ $0 \rightarrow l \rightarrow 16$	$0 \rightarrow h \rightarrow 23$ $0 \rightarrow k \rightarrow 5$ $0 \rightarrow l \rightarrow 16$
No. of standard reflections	2	2	2
Frequency of standard reflections	Every 100 reflections	Every 100 reflections	Every 100 reflections
Intensity decay (%)	0	0	0
Refinement			
Refinement on	F^2	F^2	F^2
$R(F^2)$	0.0679	0.0476	0.0342
$wR(F^2)$	0.0733	0.0552	0.0405
S	1.0428	1.0650	1.0436
No. of reflections used in refinement	996	1932	1484
No. of parameters used	83	271	271
H-atom treatment	Refined	Refined	Refined
Weighting scheme	$w = 1/[\sigma^2(F) + 0.0004F^2]$	$w = 1/[\sigma^2(F) + 0.0004F^2]$	$w = 1/[\sigma^2(F) + 0.0004F^2]$
$(\Delta/\sigma)_{max}$	0.01	0.01	0.01
Extinction method	Type I, isotropic	Type I, isotropic	Type I, isotropic
Extinction coefficient	36 (2) × 10^2	39 (1) ×10^2	51 (1) ×10^2
Source of atomic scattering factors	*International Tables for Crystallography* (1995, Vol. C)	*International Tables for Crystallography* (1995, Vol. C)	*International Tables for Crystallography* (1995, Vol. C)

scans. Integrated intensities I_o and variances $\sigma^2(I_o)$ were derived from the scan profiles as described previously (McMullan *et al.*, 1979). Lorentz factors were applied, as well as an analytical absorption correction (de Meulenaer & Tompa, 1965; Templeton & Templeton, 1973). The structure model was refined based on all independent F_o^2 values using *UPALS* (Lundgren, 1982). The atomic positions determined by X-ray diffraction† were used as a starting structure. The scale factor was varied,

† The X-ray structure was first redetermined at 163 K. Details are given in the supplementary data for this paper available from the IUCr electronic archives (Reference: BK0051). Services for accessing these data are described at the back of the journal.

Table 2. *Fractional atomic coordinates*

	x	*y*	*z*
200 K			
N1	0.1850 (2)	1/4	0.0990 (1)
N2	0.4610 (2)	1/4	0.8044 (1)
Be	0.2505 (2)	1/4	0.4184 (1)
F1	0.0531 (3)	1/4	0.3817 (3)
F2	0.2747 (3)	1/4	0.5639 (2)
F3	0.3354 (2)	0.0348 (3)	0.3638 (2)
H1	0.3137 (7)	1/4	0.1244 (6)
H2	0.0996 (9)	1/4	0.1711 (7)
H3	0.1639 (6)	0.1137 (9)	0.0497 (7)
H4	0.4897 (10)	1/4	0.7106 (5)
H5	0.5686 (7)	1/4	0.8596 (7)
H6	0.3854 (8)	0.1174 (8)	0.8238 (4)
163 K			
N11	0.2188 (2)	0.2600 (3)	0.0990
N12	0.4691 (2)	0.2527 (2)	0.3978 (1)
N21	0.3534 (2)	0.2562 (2)	0.8015 (3)
N22	0.6025 (2)	0.2404 (3)	0.6957 (3)
Be1	0.2509 (2)	0.2536 (3)	0.4161 (3)
Be2	0.5008 (2)	0.2553 (3)	0.0785 (4)
F11	0.1534 (3)	0.2299 (6)	0.3769 (6)
F12	0.2584 (3)	0.2867 (6)	0.5617 (4)
F13	0.2989 (2)	0.0333 (5)	0.3792 (5)
F14	0.2903 (2)	0.4609 (5)	0.3490 (4)
F21	0.4026 (3)	0.2750 (7)	0.1231 (6)
F22	0.5084 (3)	0.2235 (6)	−0.0674 (4)
F23	0.5485 (3)	0.4767 (6)	0.1175 (5)
F24	0.5417 (3)	0.0452 (6)	0.1443 (5)
H111	0.2820 (6)	0.2840 (15)	0.1285 (10)
H112	0.1773 (6)	0.2828 (14)	0.1732 (10)
H113	0.2137 (6)	0.0995 (12)	0.0681 (11)
H114	0.2050 (4)	0.3645 (10)	0.0218 (6)
H121	0.5342 (4)	0.2658 (11)	0.3743 (10)
H122	0.4267 (7)	0.2783 (16)	0.3255 (11)
H123	0.4604 (4)	0.0883 (9)	0.4239 (7)
H124	0.4546 (5)	0.3666 (15)	0.4646 (10)
H211	0.3720 (5)	0.2607 (17)	0.7123 (7)
H212	0.4091 (6)	0.2233 (15)	0.8513 (10)
H213	0.3032 (3)	0.1444 (9)	0.8207 (6)
H214	0.3257 (7)	0.4022 (14)	0.8282 (8)
H221	0.6125 (7)	0.2383 (12)	0.7935 (8)
H222	0.6563 (6)	0.2190 (15)	0.6382 (10)
H223	0.5583 (8)	0.1183 (17)	0.6792 (9)
H224	0.5849 (5)	0.4021 (10)	0.6796 (8)
20 K			
N11	0.2196 (1)	0.2666 (3)	0.0990
N12	0.4712 (1)	0.2538 (2)	0.3941 (1)
N21	0.3510 (1)	0.2600 (2)	0.7972 (2)
N22	0.6007 (1)	0.2369 (2)	0.6937 (2)
Be1	0.2517 (2)	0.2578 (2)	0.4152 (2)
Be2	0.5029 (1)	0.2574 (2)	0.0774 (2)
F11	0.1544 (2)	0.2247 (4)	0.3718 (3)
F12	0.2565 (1)	0.2991 (5)	0.5624 (3)
F13	0.3028 (1)	0.0366 (3)	0.3832 (3)
F14	0.2905 (1)	0.4680 (4)	0.3475 (3)
F21	0.4054 (2)	0.2905 (5)	0.1265 (3)
F22	0.5049 (2)	0.2173 (4)	−0.0687 (3)
F23	0.5540 (1)	0.4773 (4)	0.1097 (3)
F24	0.5421 (1)	0.0466 (4)	0.1451 (3)
H111	0.2832 (3)	0.2959 (10)	0.1288 (6)
H112	0.1754 (4)	0.2971 (11)	0.1708 (5)
H113	0.2151 (3)	0.0991 (10)	0.0735 (5)
H114	0.2054 (3)	0.3706 (8)	0.0213 (4)

Table 2 (*cont.*)

	x	*y*	*z*
H121	0.5369 (3)	0.2753 (8)	0.3712 (6)
H122	0.4319 (3)	0.2792 (9)	0.3164 (5)
H123	0.4622 (3)	0.0894 (9)	0.4226 (5)
H124	0.4534 (2)	0.3611 (7)	0.4672 (4)
H211	0.3634 (5)	0.2620 (7)	0.7056 (5)
H212	0.4066 (3)	0.2192 (9)	0.8479 (5)
H213	0.2997 (2)	0.1500 (8)	0.8156 (4)
H214	0.3332 (3)	0.4222 (8)	0.8244 (4)
H221	0.6183 (4)	0.2235 (10)	0.7903 (6)
H222	0.6563 (3)	0.1994 (11)	0.6397 (5)
H223	0.5494 (2)	0.1289 (7)	0.6742 (4)
H224	0.5835 (3)	0.4013 (9)	0.6752 (5)

together with positional and anisotropic displacement parameters for all atoms and an isotropic type I extinction parameter (Becker & Coppens, 1974). Scattering lengths used in the refinements were N 9.36, Be 7.79, F 5.654 and H −3.7406 fm (Sears, 1995). The final difference Fourier map did not show significant positive or negative peaks at any of the three temperatures. The experimental data are listed in Table 1 and fractional atomic coordinates in Table 2.

3. Results and discussion

The bond lengths and angles of the BeF_4^{2-} ions from the three neutron determinations are listed in Table 3. The Be—F bond lengths at 200 K vary from 1.524 (3) to 1.535 (3) Å and the F—Be—F angles vary from 108.2 (1) to 111.3 (2)°. The corresponding values for the room-temperature X-ray structure (Garg & Srivastava, 1979) are very similar: 1.522 (6)–1.535 (4) Å and 108.4 (2)–111.0 (5)°. Both these tetrahedra are quite regular with mean sides 1.531 Å and mean angles 109.5°. These values also agree well with those from other crystal structures involving BeF_4^{2-} ions (Vicat *et al.*, 1974; Le Roy & Aleonard, 1972).

In the ferroelectric phase the nonequivalent BeF_4^{2-} tetrahedra become somewhat less regular. If the differences between the maximum and minimum bond lengths and angles of these tetrahedra are defined as Δ_l and Δ_a, respectively, then at 163 K, for $Be1F_4$, Δ_l = 0.009 Å and Δ_a = 4.3°; for $Be2F_4$, Δ_l = 0.014 Å and Δ_a = 4.6°.† These may be compared with the corresponding values (X-ray structure at 133 K) of Onodera & Shiozaki (1979): for $Be1F_4$, Δ_l = 0.088 Å [1.507 (6)–1.595 (6) Å] and Δ_a = 10.2° [105.5 (3)–115.7 (4)°]; for $Be2F_4$, Δ_l = 0.063 Å [1.513 (6)–1.576 (6) Å] and Δ_a = 6.7° [106.8 (3)–113.5 (3)°]. The distortions here appear larger and dissimilar for the two ions. In our 20 K structure for $Be1F_4$, Δ_l = 0.022 Å and Δ_a = 5.3°; for $Be2F_4$ the corresponding values are 0.029 Å and 5.3°, which are similar to those obtained at 163 K.

† The X-ray structure at 163 K also indicates similar slight distortions in both BeF_4^{2-} ions.

The bond lengths and angles for the ammonium ions from the three neutron determinations are included in Table 3. In the 200 K structure, for the $N1H_4$ ion the shortest and longest N—H lengths are 0.964 (6) and 1.004 (5) Å, and the smallest and largest H—N—H angles are 107.3 (4) and 115.4 (6)°, while for the $N2H_4$ ion the corresponding bond lengths are 0.985 (6) and 1.000 (5) Å, and the angles are 108.9 (4) and 112.8 (6)°. In the room-temperature structure determination by Garg & Srivastava (1979), as well as the structure by Onodera & Shiozaki (1979), the bond lengths vary from 0.72 to 1.01 Å and the bond angles from 101 to 123°. However, the mean N—H bond length and mean H—N—H angle in both cases are 0.87 Å and 109°, respectively. The H atoms have been assigned displacement parameters of the associated N atoms in both determinations and thus these are not of much significance. Onodera & Shiozaki (1979), however, considered one ammonium ion to be somewhat disordered, because the corresponding electron distribution is more diffuse. The mean H—N—H angle found from the neutron determination is 110.4° and the N—H length is 0.989 Å, which is more than 0.1 Å longer than in the X-ray structures. This is in good agreement with the N—H length of 0.97 Å and H—N—H angle of 109.3° reported by Schlemper & Hamilton (1966) from their neutron structure of ammonium sulfate.† No indication of disorder was seen in the H-atom positions in the present work.

At 163 K the four NH_4^+ ions have an overall mean N—H bond length of 1.004 Å (maximum s.u. = 0.011 Å); the mean angle is 109.4° (maximum s.u. = 0.9°). The shortest and longest N—H bond lengths are 0.971 (8) and 1.033 (6) Å; the variation in bond angles is 105.0 (8)–118.6 (8)°. At 20 K the neutron structure gives an overall mean N—H distance of 1.018 Å (maximum s.u. = 0.007 Å); the mean angle is 109.5° (maximum s.u. = 0.6°) for all four ions. The shortest and longest N—H bond lengths are 0.971 (6) and 1.043 (7) Å; the variation in angles is 107.2 (4)–111.9 (4)°. It may be noted that the

Table 3. *Selected geometric parameters (Å, °)*

	200 K	163 K	20 K
Be1—F11	1.535 (3)	1.526 (6)	1.539 (3)
Be1—F12	1.524 (3)	1.533 (6)	1.553 (4)
Be1—F13	1.526 (2)	1.531 (4)	1.542 (3)
Be1—F14		1.524 (4)	1.533 (3)
Be2—F21		1.550 (6)	1.560 (3)
Be2—F22		1.536 (6)	1.539 (4)
Be2—F23		1.540 (5)	1.537 (3)
Be2—F24		1.539 (4)	1.538 (3)
N11—H111	1.004 (5)	1.008 (9)	1.018 (5)
N11—H112	0.988 (7)	1.002 (10)	1.014 (6)
N11—H113	0.964 (6)	0.999 (8)	1.019 (6)
N11—H114		1.033 (6)	1.033 (5)
N12—H121		1.012 (7)	1.020 (5)
N12—H122		0.997 (11)	1.012 (6)
N12—H123		1.012 (6)	1.017 (5)
N12—H124		0.989 (10)	1.022 (5)
N21—H211	1.000 (5)	0.971 (8)	0.971 (6)
N21—H212	0.993 (6)	1.003 (10)	1.015 (5)
N21—H213	0.985 (6)	1.020 (5)	1.023 (4)
N21—H214		0.993 (9)	1.027 (5)
N22—H221		1.030 (9)	1.043 (7)
N22—H222		1.012 (10)	1.028 (5)
N22—H223		0.993 (11)	1.017 (4)
N22—H224		1.001 (6)	1.016 (5)
F11—Be1—F12	111.3 (2)	110.3 (3)	110.6 (2)
F11—Be1—F13	108.2 (1)	107.9 (3)	107.6 (2)
F11—Be1—F14	108.6 (1)	108.8 (3)	109.1 (2)
F12—Be1—F13		108.7 (3)	108.7 (2)
F12—Be1—F14		108.9 (3)	108.1 (2)
F13—Be1—F14		112.2 (3)	112.8 (2)
F21—Be2—F22		112.1 (3)	111.1 (2)
F21—Be2—F23		107.5 (3)	107.0 (2)
F21—Be2—F24		107.8 (3)	108.0 (2)
F22—Be2—F23		108.3 (3)	109.5 (2)
F22—Be2—F24		109.2 (3)	108.8 (2)
F23—Be2—F24		112.0 (3)	112.5 (2)
H111—N11—H112	115.4 (6)	109.4 (8)	111.0 (5)
H111—N11—H113	107.4 (3)	107.6 (7)	107.6 (4)
H111—N11—H114	107.3 (4)	110.1 (7)	109.1 (4)
H112—N11—H113		109.1 (8)	108.6 (5)
H112—N11—H114		113.3 (7)	110.0 (4)
H113—N11—H114		107.1 (7)	110.6 (4)
H121—N12—H122		115.0 (8)	111.0 (4)
H121—N12—H123		105.2 (5)	108.2 (4)
H121—N12—H124		109.3 (7)	110.4 (4)
H122—N12—H123		105.4 (7)	107.2 (4)
H122—N12—H124		106.8 (8)	110.6 (4)
H123—N12—H124		115.3 (7)	109.3 (4)
H211—N21—H212	112.8 (6)	105.1 (8)	110.8 (6)
H211—N21—H213	108.9 (4)	114.7 (7)	109.6 (5)
H211—N21—H214	110.7 (4)	111.4 (8)	108.0 (4)
H212—N21—H213		113.0 (6)	111.9 (4)
H212—N21—H214		111.8 (8)	106.8 (4)
H213—N21—H214		101.1 (7)	109.6 (4)
H221—N22—H222		117.9 (9)	107.8 (5)
H221—N22—H223		105.0 (8)	109.7 (4)
H221—N22—H224		102.4 (7)	108.6 (4)
H222—N22—H223		110.0 (8)	111.8 (4)
H222—N22—H224		103.3 (7)	107.8 (5)
H223—N22—H224		118.6 (8)	111.1 (4)

† Ammonium sulfate (AS) is isostructural with AFB at room temperature, where both compounds are paraelectric. The space group in each case changes from *Pnma* to $Pna2_1$ upon cooling into the ferroelectric phase. The transition temperature in AS is 223 K compared with 176 K in AFB and both ferroelectrics have small values of spontaneous polarization, 0.6 μC cm^{-2} for AS compared with 0.22 μC cm^{-2} for AFB. Both have small peak values for the dielectric and Curie constants at T_c. There are, however, significant differences. There is a drastic change in polarization at the transition in AS; the unit cell also changes abruptly and the crystal breaks, unless the temperature change is very slow and the crystals very thin. These changes are smooth through the transition in AFB. There is no superlattice and doubling of the *a* axis in AS at the transition, as is the case in AFB. The specific heat shows two typical lambda-point anomalies (at 223 and 225 K) in AS, whereas AFB shows only one anomaly at the transition. There is a double hysteresis loop in AFB just before transition, but only one such loop in AS. There is also no intermediate paraelectric phase in AS. Schlemper & Hamilton (1966) have determined the structure of AS in the ferroelectric phase and they attribute the transition to changes in hydrogen bonding. However, it appears that it may not be possible to understand all of the differences in the physical behavior of AS and AFB purely on the basis of their respective hydrogen-bonding schemes.

angular distortions at 20 K are less pronounced than at 163 K and the N—H bond lengths are slightly, but systematically, increased at lower temperatures. This is to be expected, as none of the bond lengths reported above are corrected for the anisotropic thermal motion of the atoms.

The structures in the paraelectric phase (200 K) and the ferroelectric phase (163 and 20 K), as viewed down the *b* axis, are shown in Fig. 1. This figure also shows the large anisotropic thermal motion of atoms at 200 K, which decreases upon cooling and becomes quite small at 20 K. One of the H atoms that lies near $y = \frac{1}{4}$, H211,

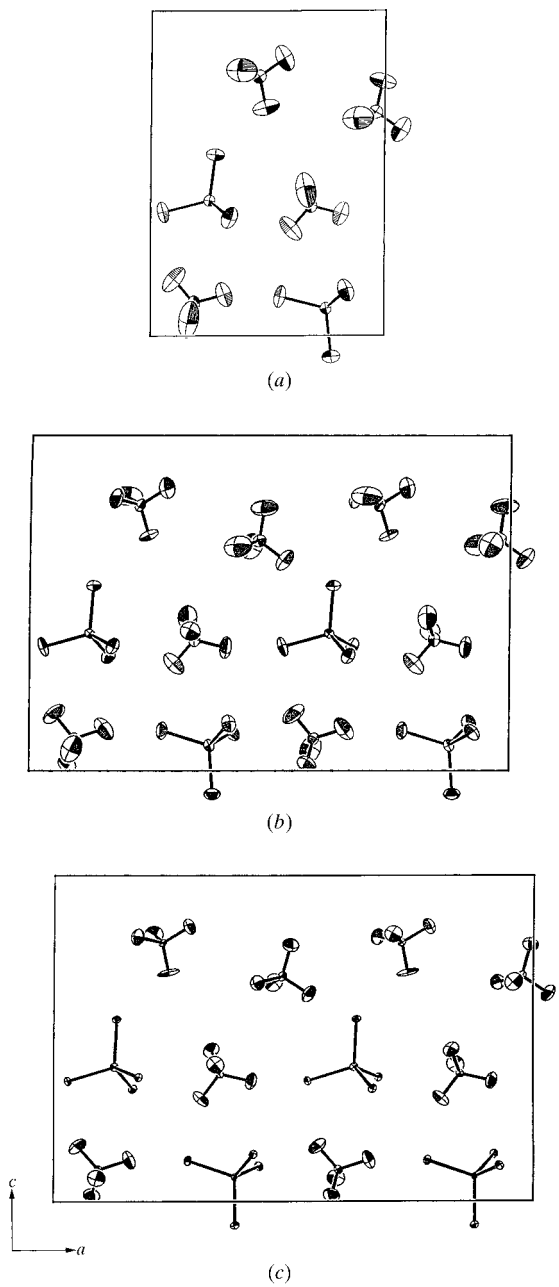

Fig. 1. Representation down the *b* axis (*a*) at 200 K, (*b*) at 163 K and (*c*) at 20 K. The view is from infinity, so that one H(F) atom of each ion is hidden. Only the ions near the plane $y = 0.25$ are shown. The unit cell at 163 and 20 K is shifted by (0.125 0.0 0.0) to correspond to the unit cell at 200 K. Ellipsoids are shown at 50% probability (Johnson, 1976). The larger ellipsoids correspond to the H atoms of the cations.

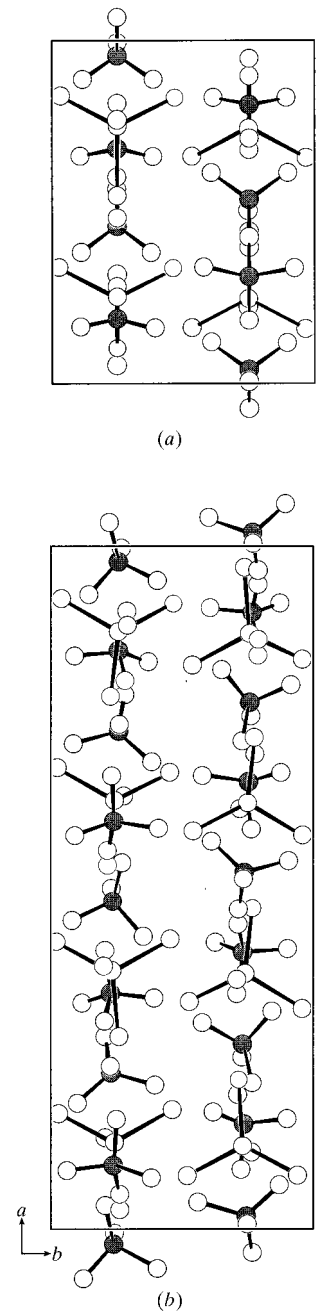

Fig. 2. View down the *c* axis (*a*) at 200 K and (*b*) at 163 K, showing the shifts from the mirror planes $y = 0.25$ and 0.75. The unit cell at 163 K is shifted by (0.125 0.0 0.0) to correspond to the unit cell at 200 K. The N atoms are shaded.

has an unusually large U^{22} value at 163 and 20 K. Figs. 2(*a*) and 2(*b*) show the structures in the paraelectric and ferroelectric phases as viewed down the *c* axis. Thermal motion has been omitted for clarity in these latter figures. It will be noticed that on going through the phase transition both the BeF_4^{2-} and NH_4^+ tetrahedra rotate as well as shift from the mirror planes at $y = \frac{1}{4}$ and $\frac{3}{4}$ of the paraelectric phase. This twist in the tetrahedra causes distortions that are more pronounced for NH_4^+ ions than BeF_4^{2-} ions. The twist and distortions give rise to stronger hydrogen-bonding interactions and stabilize the structure. Any contributions to the distortions that are due to anisotropy of the thermal motion will be diminished at lower temperatures, away from the transition temperature, *e.g.* 20 K. The distortions present here are mainly due to the requirements of the hydrogen-bonding scheme and hence are less severe than at 163 K, which is below, but close to, the transition temperature.

Fig. 3 shows a hydrogen-bonding scheme in which an attempt has been made to link all F atoms. This requires an H···F distance limit of 2.45 Å. Obviously, many of these interactions are very weak. To consider only stronger interactions, H···F < 2.1 Å may be chosen as the criterion. This is almost equivalent to the van der Waals contact-distance cutoff of N···F < 2.85 Å introduced by Pimentel & McClellan (1960). The strong bonds are indicated with open lines in Fig. 3 and the others by thin solid lines. At 200 K, in the paraelectric phase, there is one such stronger bond for $N1H_4$ and two for $N2H_4$. At 163 K, there are four such bonds for the $N22H_4$ ion and three for each of the other three ammonium ions. At 20 K, due to a small rotation, one of these bonds involving $N21H_4$ falls slightly above the 2.1 Å cutoff. These stronger hydrogen bonds at all three temperatures are listed in Table 4.

The difference between the paraelectric phase and the ferroelectric phase occurs mainly along the polar *c* axis. In the ferroelectric phase the ammonium ions move ∼ 0.03 Å closer to the nearest tetrafluoroberyllate ions within chains of molecules. The chains themselves move slightly relative to one another. The Be···Be distances in this way are increased by ∼ 0.010 Å. According to Hoshino *et al.* (1958) there is a small spontaneous polarization (0.22 μC cm^{-2}). This would correspond to a shift of ∼ 0.008 Å of the ions in the cell, in good agreement with the average observed shift of BeF_4^{2-} relative to the NH_4^+ ions of 0.007 Å. The shifts of the individual ammonium ions virtually cancel one another.

Owing to the relative movement of the ammonium ions, and the rotations of all ions, upon going through the phase transition several hydrogen bonds become slightly shorter, while one becomes slightly longer. Thus, the N1···F1 distance goes from 2.779 (2) Å at 200 K to 2.805 (3) and 2.760 (3) Å in the corresponding N11···F21 and N12···F11 hydrogen bonds at 20 K, and

Table 4. *Hydrogen-bonding geometry (Å, °)*

200 K

D—H···*A*	*D*—H	H···*A*	*D*···*A*	*D*—H···*A*
N1—H1···F1^{i}	1.004 (5)	1.804 (6)	2.779 (2)	162.7 (6)
N2—H5···F2^{ii}	0.993 (6)	1.744 (6)	2.731 (3)	171.9 (6)
N2—H6···F3^{iii}	0.986 (5)	1.933 (6)	2.857 (2)	155.0 (5)

Symmetry codes: (i) $\frac{1}{2}+x, \frac{1}{2}-y, \frac{1}{2}-z$; (ii) $\frac{1}{2}+x, y, \frac{3}{2}-z$; (iii) $\frac{1}{2}-x, -y, \frac{1}{2}+z$.

163 K

D—H···*A*	*D*—H	H···*A*	*D*···*A*	*D*—H···*A*
N11—H111···F21	1.008 (9)	1.813 (10)	2.774 (5)	158.0 (9)
N11—H113···F12^{i}	0.999 (8)	1.887 (8)	2.829 (4)	156.0 (9)
N11—H114···F13^{ii}	1.033 (6)	1.787 (8)	2.810 (5)	169.6 (5)
N12—H121···F11^{iii}	1.011 (7)	1.790 (8)	2.779 (5)	164.7 (9)
N12—H123···F22^{iv}	1.012 (6)	1.893 (7)	2.842 (4)	154.8 (6)
N12—H124···F23^{v}	0.989 (10)	1.840 (11)	2.799 (5)	162.3 (8)
N21—H212···F22^{vi}	1.003 (10)	1.715 (10)	2.705 (5)	168.6 (8)
N21—H213···F14^{vii}	1.020 (5)	1.795 (6)	2.812 (4)	176.1 (5)
N21—H214···F11^{viii}	0.993 (9)	2.016 (9)	2.894 (4)	146.2 (9)
N21—H214···F13^{viii}	0.993 (9)	2.092 (11)	2.921 (4)	139.8 (8)
N22—H222···F12^{iii}	1.012 (10)	1.728 (10)	2.730 (5)	169.1 (9)
N22—H223···F24^{iv}	0.993 (11)	1.819 (11)	2.792 (4)	165.7 (9)
N22—H224···F21^{v}	1.001 (6)	1.996 (7)	2.948 (4)	158.0 (7)

Symmetry codes: (i) $\frac{1}{2}-x, y-\frac{1}{2}, z-\frac{1}{2}$; (ii) $\frac{1}{2}-x, \frac{1}{2}+y, z-\frac{1}{2}$; (iii) $\frac{1}{2}+x, \frac{1}{2}-y, z$; (iv) $1-x, -y, \frac{1}{2}+z$; (v) $1-x, 1-y, \frac{1}{2}+z$; (vi) $x, y, 1+z$; (vii) $\frac{1}{2}-x, y-\frac{1}{2}, \frac{1}{2}+z$; (viii) $\frac{1}{2}-x, \frac{1}{2}+y, \frac{1}{2}+z$.

20 K

D—H···*A*	*D*—H	H···*A*	*D*···*A*	*D*—H···*A*
N11—H111···F21	1.018 (9)	1.833 (5)	2.805 (3)	158.5 (5)
N11—H113···F12^{i}	1.019 (8)	1.813 (7)	2.789 (4)	159.3 (4)
N11—H114···F13^{ii}	1.033 (5)	1.740 (5)	2.767 (3)	172.2 (4)
N12—H121···F11^{iii}	1.021 (5)	1.763 (5)	2.760 (3)	164.5 (5)
N12—H123···F22^{iv}	1.017 (5)	1.866 (6)	2.811 (3)	153.1 (4)
N12—H124···F23^{v}	1.022 (5)	1.762 (5)	2.767 (3)	166.6 (3)
N21—H212···F22^{vi}	1.015 (5)	1.711 (5)	2.708 (3)	166.6 (5)
N21—H213···F14^{vii}	1.023 (4)	1.754 (6)	2.777 (3)	178.4 (4)
N21—H214···F11^{viii}	1.027 (5)	1.849 (5)	2.833 (3)	159.1 (4)
N21—H214···F13^{viii}	1.027 (5)	2.232 (5)	2.958 (2)	126.3 (4)
N22—H222···F12^{iii}	1.028 (5)	1.704 (5)	2.715 (3)	166.1 (6)
N22—H223···F24^{iv}	1.017 (4)	1.742 (4)	2.757 (3)	177.1 (4)
N22—H224···F21^{v}	1.016 (5)	1.883 (6)	2.858 (3)	159.7 (4)

Symmetry codes: (i) $\frac{1}{2}-x, y-\frac{1}{2}, z-\frac{1}{2}$; (ii) $\frac{1}{2}-x, \frac{1}{2}+y, z-\frac{1}{2}$; (iii) $\frac{1}{2}+x, \frac{1}{2}-y, z$; (iv) $1-x, -y, \frac{1}{2}+z$; (v) $1-x, 1-y, \frac{1}{2}+z$; (vi) $x, y, 1+z$; (vii) $\frac{1}{2}-x, y-\frac{1}{2}, \frac{1}{2}+z$; (viii) $\frac{1}{2}-x, \frac{1}{2}+y, \frac{1}{2}+z$.

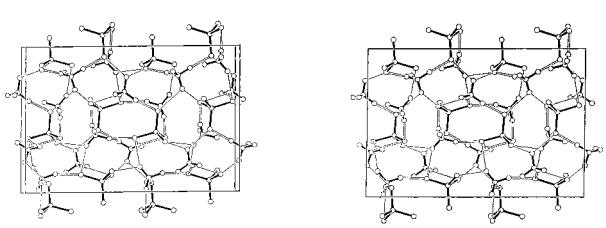

Fig. 3. Stereoview down the *b* axis, with the origin at the lower left and the *a* axis pointing to the right, showing hydrogen bonding in AFB at 163 K. Hydrogen bonds with H···F < 2.10 Å, also listed in Table 4, are indicated by double lines. Weaker interactions, with 2.10 Å < H···F < 2.45 Å, are indicated by single lines.

N2···F2 goes from 2.730 (2) Å at 200 K to 2.708 (3) and 2.713 (3) Å in the corresponding N21···F22 and N22···F12 hydrogen bonds at 20 K. Thus, at 20 K the two shortest hydrogen bonds in AFB, N21···F22 2.708 (3) and N22···F12 2.713 (3) Å, are both ~ 0.02 Å shorter than the shortest bond at 200 K, N2···F2 2.730 (2) Å.

4. Conclusions

Going from the paraelectric to the ferroelectric phase, both the BeF_4^{2-} and the NH_4^+ ions rotate and shift from the mirror planes of the paraelectric phase. This results in the removal of the mirror-plane symmetry and the formation of a superlattice with the *a* axis doubled. Along the polar *c* axis, the NH_4^+ ions move towards the BeF_4^{2-} ions within chains of molecules and the chains move slightly relative to one another. The rotations and translations give rise to stronger hydrogen-bonding interactions. An average shift of 0.007 Å of the BeF_4^{2-} ions relative to the NH_4^+ ions gives rise to the small spontaneous polarization (0.22 $\mu C\ cm^{-2}$; Hoshino *et al.*, 1958). Under these circumstances the NH_4^+ ions may also be expected to have some dipole moment. These ions are held in particular orientations as a result of the stronger hydrogen-bonding interactions. Any contributions to the distortions in the BeF_4^{2-} and NH_4^+ tetrahedra that are due to the anisotropic thermal motion of the atoms will be diminished at temperatures lower than the transition temperature, and the remaining distortions are then mainly due to the requirements of the hydrogen-bonding scheme. At such temperatures these tetrahedra are generally less distorted than at the transition temperature, but more so than those in the paraelectric phase.

We would like to thank C. Koehler III for technical assistance. Work at Brookhaven National Laboratory was performed under contract DE-AC02-98CH10886 with the US Department of Energy and supported by its Office of Basic Energy Sciences. The redetermination of the X-ray structure at 163 K was carried out by RCS at the University of Pittsburgh, Department of Crystallography, where he served as a visiting professor.

References

Becker, P. J. & Coppens, P. (1974). *Acta Cryst.* A**30**, 129–144.
Garg, A. & Srivastava, R. C. (1979). *Acta Cryst.* B**35**, 1429–1432.
Hoshino, S., Vedam, K., Okaya,Y. & Pepinsky, R. (1958). *Phys. Rev.* **112**, 405–409.
Iizumi, M. & Gesi, K. (1977). *Solid State Commun.* **22**, 37–39.
Johnson, C. K. (1976). *ORTEP*II. Report ORNL-5138. Oak Ridge National Laboratory, Tennessee, USA.
Kydon, D. W., Petch, H. E. & Pinter, M. (1969). *J. Chem. Phys.* **51**, 487–489.
Le Roy, J. & Aleonard, S. (1972). *Acta Cryst.* B**28**, 1383–1387.
Levanyuk, A. P. & Sannikov, D. G. (1969). *JETP Sov. Phys.* **28**, 134–137.
Lundgren, J.-O. (1982). *Crystallographic Computer Programs*. Report UUIC-B13-4-05. Institute of Chemistry, University of Uppsala, Sweden.
McMullan, R. K., Epstein, J., Ruble, J. R. & Craven, B. M. (1979). *Acta Cryst.* B**35**, 688–670.
Makita, Y. & Yamauchi, Y. (1974). *J. Phys. Soc. Jpn*, **37**, 1470–1474.
Meulenaer, J. de & Tompa, H. (1965). *Acta Cryst.* **19**, 1014–1018.
Ohshima, H. & Nakamura, E. (1966). *J. Phys. Chem.* **27**, 481–484.
Onodera, A. & Shiozaki, Y. (1979). *J. Phys. Soc. Jpn*, **46**, 157–166.
O'Reilly, D. E., Peterson, E. M. & Tsang, T. (1967). *Phys. Rev.* **160**, 333–336.
Pepinsky, R. & Jona, F. (1957). *Phys. Rev.* **105**, 344–347.
Pimentel, G. C. & McClellan, A. L. (1960). *The Hydrogen Bond*, p. 292. San Francisco: W. H. Freeman and Company.
Schlemper, E. O. & Hamilton, W. C. (1966). *J. Chem. Phys.* **44**, 4498–4509.
Sears, V. F. (1995). *International Tables for Crystallography*, Vol. C, pp. 383–391. Dordrecht: Kluwer Academic Publishers.
Strukov, B. A., Gavrilova, N. D. & Koptsik, V. A. (1962). *Sov. Phys. Cryst.* **7**, 182–183.
Strukov, B. A., Skomorokhova, T. L., Koptsik, V. A., Boiko, A. A. & Izrailenko, A. N. (1973). *Sov. Phys. Cryst.* **18**, 86–88.
Templeton, L. K. & Templeton, D. H. (1973). Am. Crystallogr. Assoc. Meet. Abstracts p. 143. Storrs, Connecticut, USA.
Vicat, P. J., Tranqui, D., Aleonard, S. & Richard, P. (1974). *Acta Cryst.* B**30**, 2678–2682.